Marine Pollution Bulletin 197 (2023) 115733

Contents lists available at ScienceDirect

Marine Pollution Bulletin

journal homepage: www.elsevier.com/locate/marpolbul

Seasonal distribution patterns of *Scomberomorus commerson* in the Taiwan Strait in relation to oceanographic conditions: An ensemble modeling approach

Sandipan Mondal [a,b], Ming-An Lee [a,b,c,*], Jinn-Shing Weng [d], Kennedy Edeye Osuka [e], Yu Kai Chen [d], Aratrika Ray [a]

[a] Department of Environmental Biology Fisheries Science, National Taiwan Ocean University, Keelung 202, Taiwan
[b] Center of Excellence for the Oceans, National Taiwan Ocean University, Keelung 202, Taiwan
[c] Doctoral degree program in Ocean Resource and Environmental Changes, National Taiwan Ocean University, Keelung 202, Taiwan
[d] Coastal and Offshore Resources Research Center of Fisheries Research Institute, Council of Agriculture Executive Yuan, Kaohsiung 80672, Taiwan
[e] Department of Earth, Ocean and Ecological Sciences, University of Liverpool, Liverpool L69 3BX, United Kingdom

ARTICLE INFO

Original content: 1. Spanish_Mackerel_53201_N (Reference data)

Keywords:
Ensemble modeling
Scomberomorus commerson
Seasonal variability
Single-algorithm model
Taiwan Strait

ABSTRACT

The decline in the stock of the narrow-barred Spanish mackerel in the Taiwan Strait has sparked interest in conservation efforts. To optimize conservation and restoration efforts, it is crucial to understand their habitat preference in response to changing environments. In this study, ensemble modeling was used to investigate the seasonal distribution patterns of Spanish mackerel. Winter was identified as the most productive season, followed by fall; productivity was the lowest in summer. Five single-algorithm models were developed, and on the basis of their performance, four were selected for inclusion in an ensemble species distribution model. The spatial distribution of Spanish mackerel was primarily along the latitudinal range 23°–25°N in spring and summer. However, in fall and winter, the geographical range increased toward the southern region. The findings of this study will contribute to the understanding of this specific species and the approach used in this study may be applicable to other fisheries stocks also.

1. Introduction

The Taiwan Strait, also known as the Formosa Strait, connects the southwestern East China Sea to the northeastern South China Sea between China's Fukien Province and Taiwan. Its depth is estimated to be approximately 70 m, and is currently a key a navigational route for many vessels to access ports in Northeast Asia. Furthermore, the strait has abundant marine life and high biodiversity and is ecologically and commercially critical; it was included at No. 61 in the Food and Agricultural Organization's list of major fishing regions (Mondal et al., 2023). The branching Kuroshio Current along with the South China Sea Warm Current, and the China Coastal Current significantly influences the productivity and biodiversity of the waters in the Taiwan Strait (Hobday and Pecl, 2014; Ho et al., 2016; Ju et al., 2019; Liao et al., 2019).

Scomberomorus commerson, (Family: Scombridae) is widely distributed in Southeast Asia and has high economic value in the Taiwan Strait region (Ju et al., 2020). This species is a key member of Taiwan's coastal and offshore fisheries (see Supplementary Fig. 1) (Di Natale et al., 2020), and the modest depth of the southern Taiwan Strait is a key location for catching narrow-barred Spanish mackerel, with 70 % of the total catch from the Taiwan Strait. However, the narrow-barred Spanish mackerel catch in this region greatly decreased from 6600 tons in 2002 to 517 tons in 2019 (Taiwan Fisheries Agency, 2019). This decline was attributed to overfishing and increased demand (Ju et al., 2020). Oceanographic circumstances influence the distribution of any marine species. Thus, understanding the association between oceanographic attributes and the distribution of narrow-barred Spanish mackerel is critical to facilitating the recovery of populations of this species. This knowledge could aid in the identification of previously unknown fishing areas and reduce the pressure on existing fishing grounds. (Devi et al., 2015). Therefore, examining oceanographic characteristics and their effects on the narrow-barred Spanish mackerel distribution pattern is an initial measure for effective management.

* Corresponding author at: Department of Environmental Biology Fisheries Science, National Taiwan Ocean University, Keelung 202, Taiwan.
E-mail address: malee@mail.ntou.edu.tw (M.-A. Lee).

https://doi.org/10.1016/j.marpolbul.2023.115733
Received 26 April 2023; Received in revised form 25 October 2023; Accepted 26 October 2023

Fish behavior and physiology —including feeding, metabolism, and reproduction—are sensitive to changes in ocean dynamics (Xing et al., 2022; Liu et al., 2022). For example, sea surface temperature (SST) significantly influences the abundance of narrow-barred Spanish mackerel in surface waters (Chen et al., 2021). This relationship is influenced by body temperature control and heat loss systems (Nguyen and Nguyena, 2017). Species-specific tolerances are linked to distribution boundaries, and spatial distribution is influenced by food resources (Niamaimandi et al., 2015). Sea surface chlorophyll (SSC) measures phytoplankton concentration, which attracts small fish that serve as a food source for the narrow-barred Spanish mackerel (Welliken et al., 2021). Salinity is crucial for maintaining osmotic pressure (Nguyen and Nguyena, 2017). SST influences mixed layer depth (MLD) and sea surface height (SSH) (de Boyer et al., 2004), facilitating deep-diving species like the Spanish mackerel's prey search (Lan et al., 2020). These facts highlight the importance of comprehending the effects of oceanographic conditions (Barman et al., 2023; Barman and Bora, 2021a; Barman and Bora, 2021b; Barman and Bora, 2021c) for understanding the distribution pattern of the narrow-barred Spanish mackerel.

In the above context, species distribution models (SDMs)—which are also referred to as habitat models, ecological niche models, bioclimatic envelopes, and resource selection functions—can be used for assessing the relationship between narrow-barred Spanish mackerel and their environment in the Taiwan Strait (Tikhonov et al., 2020; Li and Wang, 2013; Beale and Lennon, 2012; Robinson et al., 2011; Zimmermann et al., 2010). SDMs are mathematical models that predict and forecast species' distribution in their environment, using algorithmic representations to describe species' environmental habitats. Studies have employed arithmetic mean models and geometric mean models (Xue et al., 2017; Li et al., 2016), both of which rely on the habitat suitability index. However, these methods have drawbacks, such as their sensitivity to outliers, inability to be applied to zero and negative numbers, and are highly affected by small values in the dataset. Recent technological advances have enabled the implementation of statistical regression models with great potential, such as generalized linear models (GLMs; Azzellino et al., 2012) and generalized additive models (GAMs; Zhang et al., 2021). Other promising models include artificial intelligence models such as gradient boosting models (GBMs; Hossain et al., 2020), artificial neural networks (Ahmad, 2019), classification and regression tree (CTA) models (Youssef et al., 2016), and random forest (RF) models (Reisinger et al., 2018). SDMs are versatile tools that enhance ecological and conservation research by providing insights into species distributions, aiding in conservation planning, and supporting decision-making processes (Barry and Elith, 2006).

However, single algorithm SDMs may have limitations due to their inherent capabilities and limitations. They may not fully capture species-environment connections, which could not help to identify undiscovered fishing sites fully (Yackulic et al., 2013). Additionally, they may overfit, focusing too much on training data, resulting in suboptimal performance for species distributions beyond the training range (Pacifici et al., 2017). Furthermore, they may not adequately address uncertainty, as different algorithms can yield varying estimates of uncertainty (Barry and Elith, 2006). To overcome these limitations, ensemble methodology is often recommended (Rowden et al., 2017a, 2017b), which amalgamates multiple algorithms to enhance model efficacy and predictability. Thus, ensemble approaches have recently been widely applied through techniques such as core bagging, boosting, and stacking (Tittensor et al., 2018; Gårdmark et al., 2013). Ensemble models are thought to have superior performance to single-algorithm models and have become increasingly popular. Alabia et al. (2016) demonstrated that ensemble model can reduce prediction error variance. Thus, in the present study, ensemble habitat modeling was performed along with single-algorithm modeling.

The understanding of the relationships between the distribution of narrow-barred Spanish mackerel and oceanographic parameters is lacking because of the scarcity of high-resolution fisheries data. Previous studies have demonstrated the significant influences of oceanographic characteristics on the distribution patterns of narrow-barred Spanish mackerel in the Taiwan Strait (Chen et al., 2021) and other oceanic areas (Nguyen and Nguyena, 2017; Hu et al., 2022). The Taiwan Strait investigation only used single-algorithm model and limited fisheries data until 2016. It also lacked fishery data standardization, potentially allowing for bias due to spatial or temporal factors. The present study utilized a refined, recent narrow-barred Spanish mackerel data set with a spatial resolution of 0.1° to comprehensively understand its distribution pattern using an ensemble habitat modeling approach. The study hypothesized that the seasonal distribution of narrow-barred Spanish mackerel in Taiwan Strait is influenced by oceanographic characteristics, and that using an ensemble model offers a more comprehensive understanding than previous studies that relied on single-algorithm models. The findings of the current study could contribute to the attainment of various sustainable development goals (SDGs), including but not limited to reducing the time required for access to fishing grounds, reducing fishing intensity on the existing fishing areas, identification of new fishing grounds, enhancing profitability, identifying regions that are overexploited for future restoration efforts, and ultimately promoting sustainable fisheries. Additionally, the approach used in this study may be applicable to other fisheries stocks of the Taiwan Strait also.

Trawl nets, gillnets, drift nets, trolling lines, and longline fishing vessels are often used to capture this species (Supplementary Fig. 2). Of these methods, the gillnet is the most common, accounting for 70 % of all captures (Supplementary Fig. 3). Consequently, we exclusively concentrated on gillnet captures of this species. Gillnet vessels primarily engage in fishing activities within coastal seas and must adhere to particular criteria, including a gross registered tonnage of <100, a length of <24 m, and a width of 8 m.

2. Materials and method

A brief experimental flowchart is displayed in Fig. 1. Initially, fishery and oceanographic data were collected and rescaled using MATLAB to the same spatial and temporal grid. The final dataset was obtained by standardizing fishery data using a GLM in order to reduce data bias caused by various factors. Next, the five single-algorithm models were employed to determine the relationship between fisheries and oceanography. Before constructing an ensemble model, each single-algorithm model was validated using the root mean square error (RMSE) and mean absolute error (MAE) indices. The study area's fishery distribution was predicted using an ensemble habitat model constructed from single-algorithm models that exhibited better performance and no significant bias during validation.

2.1. Data collection

2.1.1. Fishery data

Taiwan's fisheries agency provided narrow-barred Spanish mackerel fishery data with an explicit focus on small-scale gillnet captures. The data set encompassed the period from January 2014 to December 2019. The fishing activities were limited to those in coastal waters and involved vessels with a gross registered tonnage of <100, a length of <24 m, and a width of 8 m. The monthly gillnet fishing data were from a spatial range between 22°–26°N and 117°–12°E (Supplementary Fig. 4) and had a spatial resolution of 0.1°. The logbook containing the data included various data points, including the year and month of recording, the geographical coordinates as latitude and longitude, the quantity of fish caught in kilograms, the amount of time dedicated to fishing activities in hours, the aggregate weight of the catch (without distinction between dry versus wet weight), the specific fishing gear employed, and the unique identification number assigned to the vessel. No information regarding the duration of gear soaking or the depth at which fishing occurred was available.

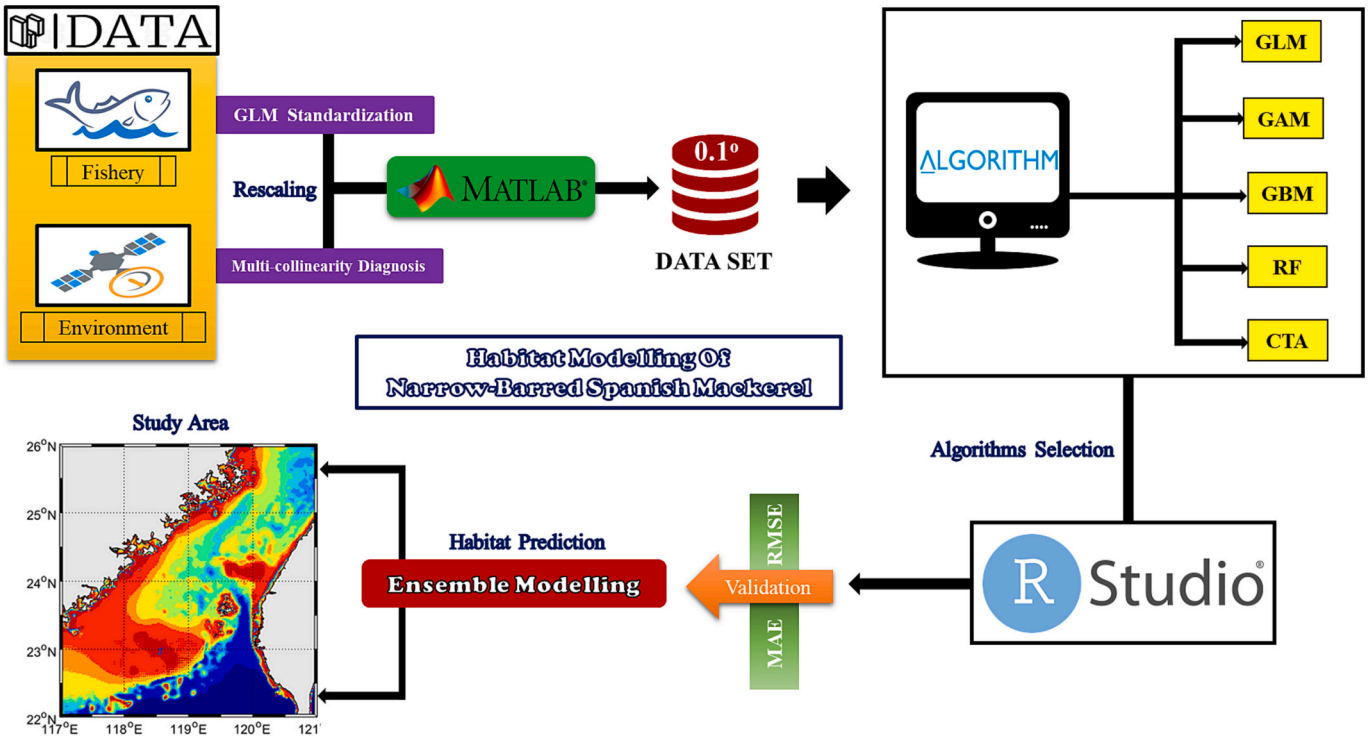

Fig. 1. Experimental flowchart.

2.1.2. Oceanographic data

Data for six oceanographic parameters—the SST, sea surface salinity (SSS), MLD, SSH, bathymetry (BAT), and SSC—were gathered from various sources. The spatiotemporal coverage of the oceanographic data and that of the fisheries data were matched through linear interpolation (a technique for fitting curves that creates new data points within the bounds of a discrete set of existing data points using linear polynomials). Linear interpolation is a simple technique and most commonly used for data matching. In the current investigation, a straight line was geometrically drawn between two points on the geographical location to achieve linear interpolation. The sources of oceanographic parameters and the source specifications are presented in Table 1.

2.2. Standardization of fishery data

The narrow-barred Spanish mackerel catch was indexed as the nominal catch per unit effort (N.CPUE). N.CPUE was calculated using the following formula (Dunn et al., 2000; Lauridsen et al., 2008):

$$\text{N.CPUE} = \frac{\text{Catch in kilogram}}{\text{Fishing effort in hours}}$$

N.CPUE was standardized using a GLM, (Hazin et al., 2007; Hinton and Maunder, 2004, and Tian et al., 2009) which, has several key advantages. This approach enables the generation of bias-filtered data, effectively mitigating the effects of various geographic (latitude and longitude), temporal (year and month), and interaction (temporal × spatial) components, (Mondal et al., 2022). Response variables can indicate the exponential distribution across several types and accommodate categorical predictors. The GLM (stat package) for standardizing N.CPUE to obtain the standardized catch per unit effort (S.CPUE) was expressed as follows:

$$\text{S.CPUE} : \text{Log}\,(\text{N.CPUE}) \sim \textit{Year} + \textit{Season} + \textit{Latitude} + \text{Longitude} + \text{Interactions}$$

Table 1
Sources of oceanographic parameters, together with the source specifications (Access Date – 12.11.2022).

Analysis	Product Name	Vertical Layer	Processing Level	Coordinate System	Oceanographic parameter	Temporal Resolution	Spatial Resolution
Global ocean eddy-resolving reanalysis[a]	GLORYS12V1	50	L4	WGS 84	SST SSS MLD SSH	Monthly	0.083°
Global ocean biogeochemical hindcast[b]	FREEGLORYS2V4	75	L4	ETRS 89	SSC	Daily	0.25°
ERDDAP[c]	SRTM30+ Version 1.0	–	–	Global	BAT	30 arc *sec*	1°

L = Level.
WGS = World Geodetic System.
ETRS = European Terrestrial Reference System.
ERDDAP = Environmental Research Division's Data Access Program.
[a] (https://resources.marine.copernicus.eu/product-detail/GLOBAL_MULTIYEAR_PHY_001_030/INFORMATION).
[b] (https://resources.marine.copernicus.eu/product-detail/GLOBAL_MULTIYEAR_BGC_001_029/INFORMATION).
[c] (https://coastwatch.pfeg.noaa.gov/erddap/griddap/usgsCeSrtm30v1.html).

Interactions investigated: year × latitude, year × longitude, and latitude × longitude. S.CPUE was only used for the following analysis.

2.3. S.CPUE variability in relation to oceanographic parameters

Initially, oceanographic characteristics were categorized into distinct ranges. The SSTs observed during the study period were between 16 and 26 °C; each 1 °C interval was considered a separate group. The SSSs observed during the study period were between 30 and 35 practical salinity units (psu); categories were at intervals of 0.5 psu. The SSC levels ranged from 0.1 to 1.8 mg m^{-3} and were categorized into groups with intervals of 0.1 mg m^{-3}. The minimum and maximum MLD values ranged from 0 to 70 m and were categorized into groups every 5 m. The SSH range over the study period was 0.4 to 0.8 m, and divisions were made into groups every 0.1 m. Finally, BAT levels ranged from 0 to 490 m and were grouped in intervals of 10 m. Once the oceanographic parameters had been categorized, S.CPUE was matched with the corresponding oceanographic parameter data with the predetermined groupings, ensuring that the S.CPUE data were accurately associated with the correct group for each oceanographic parameter. The groups with the highest S.CPUE for each parameter were then determined.

2.4. Seasonal changes in the latitudinal and longitudinal center of gravity of S. CPUE

The study months were divided into four seasons (summer, June–August; fall, September–November; winter, December–February; and spring, March–May). To better understand the seasonal spatial distribution of the fishing and the variability associated with it, the latitudinal and longitudinal centers of gravity of the Spanish mackerel S.CPUE from the gillnet capture (gravitational center) were calculated as follows (Lehodey et al., 1997):

$$G_{\text{latitude}} = (\text{Vessel location}_{\text{latitude}} \times \text{S.CPUE}_{\text{season}})/\text{S.CPUE}_{\text{season}}$$

$$G_{\text{longitude}} = \left(\text{Vessel location}_{\text{longitude}} \times \text{S.CPUE}_{\text{season}}\right)/\text{S.CPUE}_{\text{season}}$$

2.5. Collinearity analysis

If two explanatory variables have high collinearity (i.e., a strong correlation), accurately estimating the respective regression coefficients can be challenging or unfeasible. In this study, potential multicollinearity was assessed with the variance inflation factor (VIF) metric. The VIF was calculated using the "vif" function from the "car" package in the R statistical software. Oceanographic parameters with a VIF exceeding five were deemed collinear and thus eliminated from the subsequent analysis (Zuur et al., 2010). Additionally, we conducted a Pearson correlation coefficient analysis (PCCA), (Báez et al., 2020), to identify any collinearity among the explanatory factors in all potential pairwise combinations. The level of collinearity between two independent variables was measured on a scale ranging from −1 to +1. The indexing scale used in this study was partitioned into six sections. A score of 0 denoted the absence of any relationship, and a score of +1 or − 1 indicated a perfect positive or negative correlation, respectively. Scores ranging from +0.1 to +0.3 or − 0.1 to −0.3 indicated a weak positive or negative correlations, respectively. Similarly, scores ranging from +0.4 to +0.7 or − 0.4 to −0.7 were defined as moderate positive or negative correlations, respectively. Finally, scores ranging from +0.8 to +1.0 or − 0.8 to −1.0 indicated strong positive or negative correlations, respectively (Ratner, 2009). Explanatory variables with a correlation coefficient of 0.6 or greater (Zuur et al., 2010), were considered collinear and therefore eliminated from the model construction process (Lezama-Ochoa et al., 2017).

2.6. Development of single-algorithm habitat models

Five distinct algorithmic modeling strategies were employed, namely the GLM, GAM, GBM, RF, and CTA strategies. Each modeling approach was optimized using protocols specific to that method. A comprehensive model incorporating all noncollinear oceanographic factors was then constructed for each modeling technique. The explanatory variables in this study encompassed all oceanographic characteristics, and the response variable was S.CPUE. All models were constructed using packages in R. The GAM and GLM were constructed using the oceanographic parameters provided and the "mgcv" package, assuming a Gaussian distribution. A GBM was constructed using the "gbm" package, employing the Gaussian family. The optimized hyperparameters of the GBM were 100 trees, 7 layers of interaction, and a bag fraction of 0.65. The RF model was created using the Gaussian family from the "randomForest" package. The optimized hyperparameters of the RF model were 120 trees, an interaction depth of 5, and a bag fraction of 0.45. The CTA model was developed using the "rpart" program with the Gaussian family. The performance of these single-algorithm models was evaluated using the RMSE, MAE, and correlation coefficient (R), (Mondal et al., 2023). A model was deemed superior to another model if at least two of its three metrics values were superior. The model(s) with the lower performance ($R < 0.4$) was (were) excluded from the subsequent analysis. R value below 0.4 indicated weaker correlation between the observed and predicted CPUE value (Ratner, 2009).

2.7. Validation of the selected single-algorithm models

To validate the chosen single-algorithm models, the fishing data set (comprising 1112 observations) was divided into two sections: 70 % for training ($n_{70} = 779$) and 30 % ($n_{30} = 333$) for testing (Alabia et al., 2016). The "caret" package (Kuhn, 2008) was used to randomly split the data set. The same training data set was used to train all of the selected single-algorithm models. To confirm the reliability of the findings, threefold cross validation (CV) was employed. Three metrics, namely R, the RMSE, and the MAE, were calculated for each of the test and training data sets using each selected single-algorithm models. The R, RMSE and MAE were also computed during CV to assess the robustness of the results. The models had no significant bias when at least two of its three metrics values for the three CV runs and for the testing and training data sets were similar. Only single-algorithm models that met the above threshold were considered for the construction of the ensemble habitat model.

2.8. Development of ensemble habitat model

We developed an ensemble habitat model using the selected single-algorithm models to enhance the accuracy of habitat prediction and minimize bias. Ensemble models have greater resilience to noise and are less likely to be overfit than are single models. After evaluating the performance of each single-algorithm models, we constructed an ensemble model based on the weighted means of the selected single-algorithm models to analyze the habitat of the narrow-barred Spanish mackerel (Stohlgren et al., 2010; Rew et al., 2020, and Hysen et al., 2022). The performance of the ensemble habitat model was evaluated with the RMSE and MAE indices (Mondal et al., 2023).

2.9. Comparison of single-algorithm and ensemble model performance

In this study, the performance of the single-algorithm models and the ensemble model were compared using four indices: RMSE, MAE, area under curve (AUC), and true skill statistics (TSS). The AUC is independent of prevalence; it is essentially the proportion of the total area below the ROC curve within a unit square (Pearce and Ferrier, 2000). Calculating the number of false positive and true positive outcomes for various thresholds and plotting them on a square defines the ROC curve.

TSS includes sensitivity and specificity, is unaffected by prevalence, and typically follows the same trend as AUC (Charbonnel et al., 2023). The lowest RMSE and MAE values and the highest AUC and TSS values were considered as optimal. Ensemble habitat model was selected for the subsequent analysis if at least three of its four metrics values were superior of the selected single-algorithm models.

2.10. Ensemble habitat model validation and prediction

After calculating the weighted mean of the selected single-algorithm models to derive the ensemble model, we employed the "caret" package to conduct threefold CV again to validate the ensemble model. The data set was analyzed using the ensemble habitat model, and the AUC and TSS were determined. After confirming that the AUC and TSS values obtained from the threefold CV did not have any statistically significant disparities, we employed the ensemble model to predict CPUE (P.CPUE) for each season and 0.1° spatial grid. Subsequently, P.CPUE for every point within the designated research area was graphed on a spatial grid with a resolution of 0.1°, organized by season, in conjunction with S. CPUE.

- Oceanographic data interpolation (linear): MATLAB, Version 2019a
- Data standardization: R Studio, Version 3.6.0
- Development of single-algorithm habitat models: R Studio, Version 3.6.0
- Validation of the selected single-algorithm models: R Studio, Version 3.6.0
- Validation of the ensemble model and prediction: R Studio, Version 3.6.0

3. Results

3.1. S.CPUE variability in relation to oceanographic parameters

A comparison of the nominal and standardized CPUE for narrow-barred Spanish mackerel caught in various seasons is shown in Fig. 2. From 2014, CPUE decreased until 2017. No information about gillnet fishing was available for 2018. The distribution of S.CPUE in different seasons in relation to all possible pairs of oceanographic parameters is depicted in Supplementary Fig. 5. Regarding the SST, the highest S. CPUE in the winter was observed mainly in areas with SST = 16–17 °C, whereas during the summer it was at 25–26 °C (Table 2). In spring and fall, the highest S.CPUE values were obtained at SSTs of 18–19 and 22–23 °C, respectively. The SSC and MLD values associated with the highest S.CPUE were smaller in the winter than in the summer. The highest S.CPUE was observed for an MLD of 51–60 m in the winter but 21–30 m in all other seasons. The SSS value for the highest S.CPUE was 29–29.5 psu in spring; this was the lowest SSS value for the highest S. CPUE among all the seasons.

3.2. Collinearity analysis

The PCCA (Fig. 3) and VIF (Fig. 4) results revealed no significant

Table 2
Environmental preferences in different seasons.

	SST	SSC	SSS	MLD	SSH	BAT
Winter	16–17	1.2–1.3	31–31.5	0–5	0.5–0.6	51–60
Spring	18–19	0.7–0.8	29–29.5	5–10	0.4–0.5	21–30
Summer	25–26	1.3–1.4	30–30.5	10–15	0.3–0.4	21–30
Autumn	22–23	0.9–1	29.5–30	10–15	0.4–0.5	21–30

SST = Sea surface temperature; SSC = Sea surface chlorophyll; SSS = Sea surface salinity; MLD = Mixed layer depth; SSH = Sea surface height; BAT = Bathymetry.

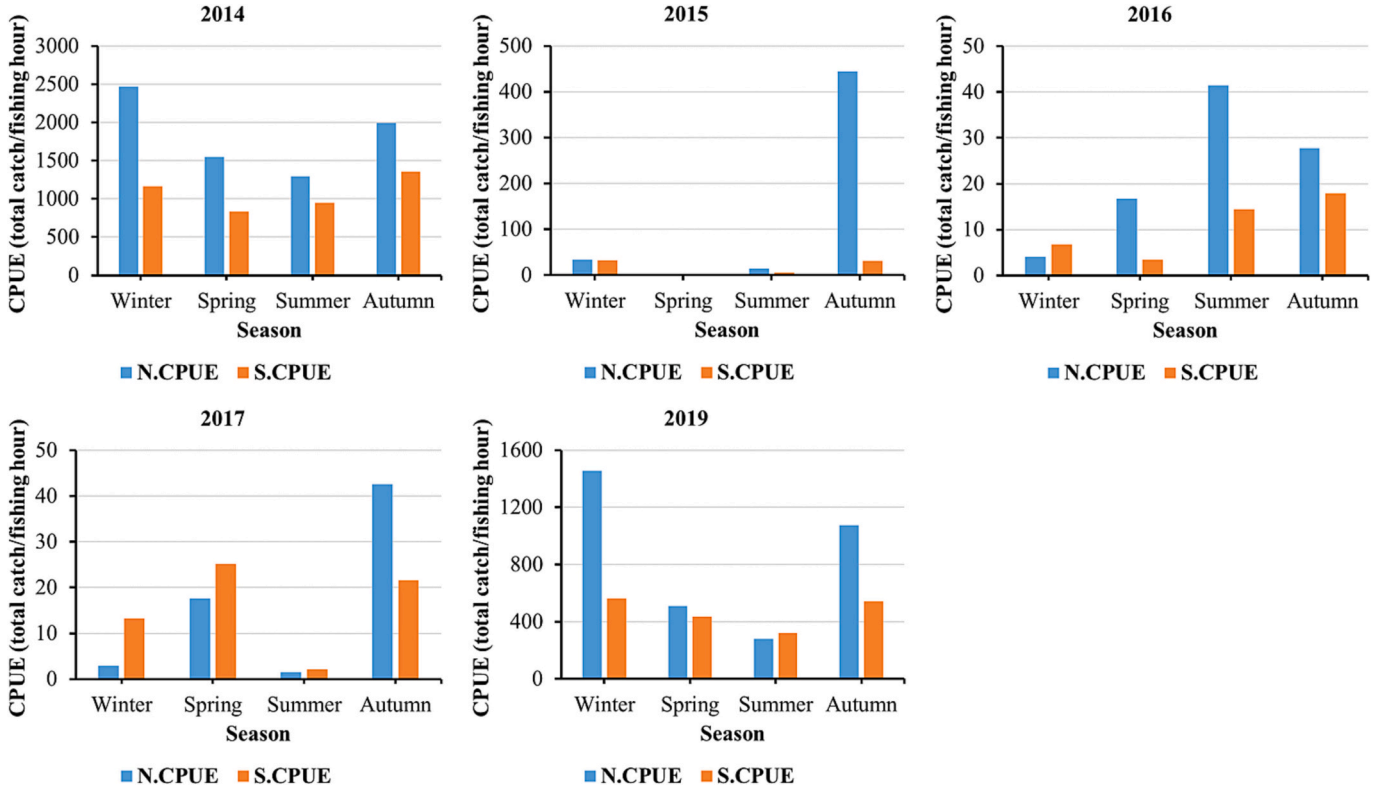

Fig. 2. Comparison of the nominal and standardized CPUE for Spanish mackerel in different years.

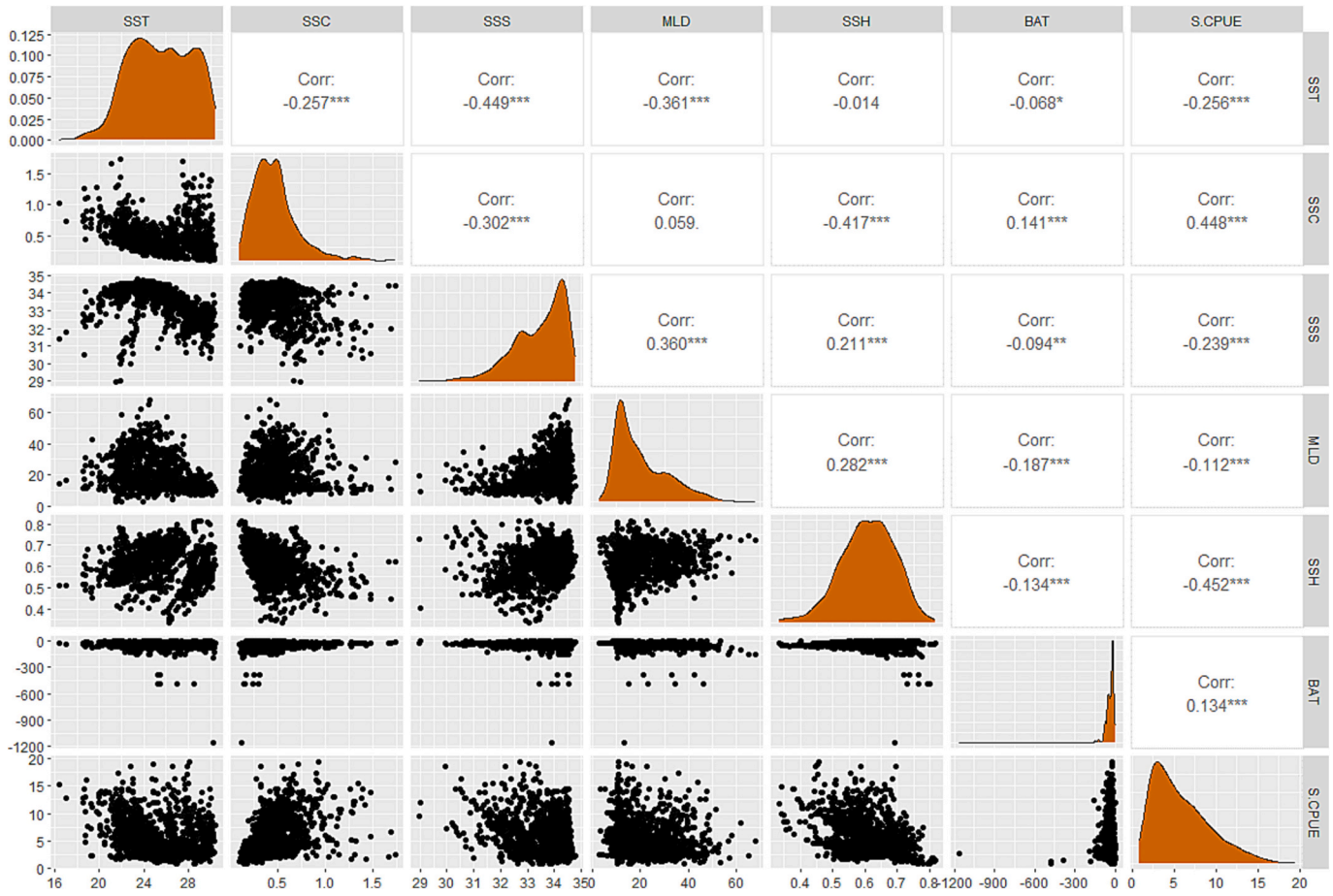

Fig. 3. PCCA of the oceanographic parameters and S.CPUE.

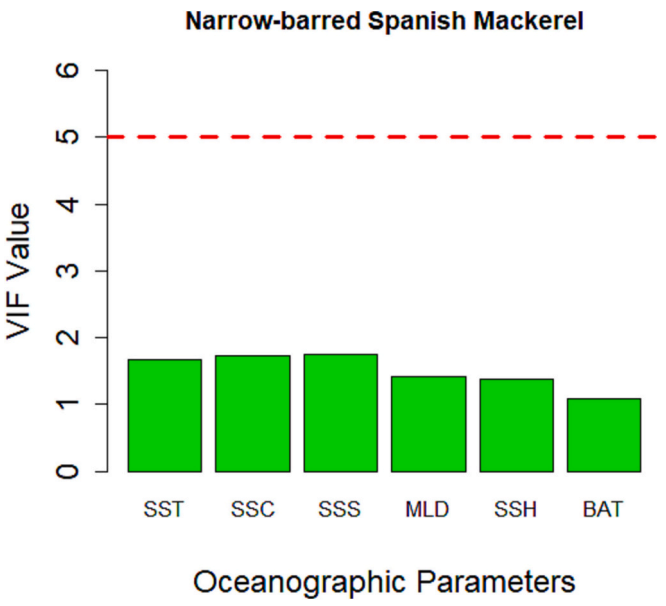

Fig. 4. VIF analysis of the oceanographic parameters to test multicollinearity. The dotted red line indicates the collinearity threshold. (For interpretation of the references to colour in this figure legend, the reader is referred to the web version of this article.)

collinearity. Therefore, all of the oceanographic parameters were considered in the subsequent analysis. The PCCA revealed that the SSH and MLD had the strongest (−0.452) and weakest (−0.112), respectively, negative correlations with S.CPUE, whereas the SSC and BAT had the strongest (0.448) and weakest (0.134), respectively, positive correlations with S.CPUE.

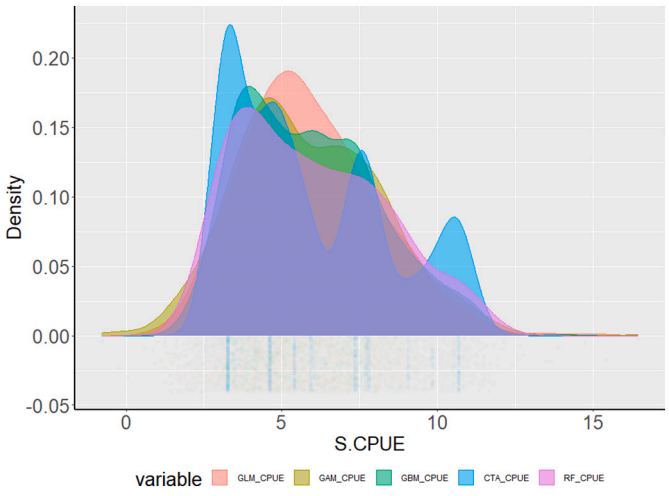

Fig. 5. Density plot for the predictions of the single-algorithm models.

3.3. Single-algorithm model performance

A comparison of the predictions of the single-algorithm models is depicted in Fig. 5 using a density plot. The shapes of the CPUE curves predicted from the single-algorithm models were as follows: the GLM, positive skew and leptokurtic; GAM, positive skew and leptokurtic; GBM, positive skew and leptokurtic; CTA model, positive skew and lepto-mesokurtic; and RF, positive skew and leptokurtic. All of the single-algorithm models' estimated CPUE curves showed that the mean was less than the median.

The predictive performance of the complete (i.e., including all oceanographic parameters) GAM, GLM, GBM, CTA, and RF model is shown in Fig. 6a. The deviance explained by the full GAM, GLM, GBM, CTA, and RF model was 45.6 %, 37.44 %, 47.13 %, 50.53 %, and 62.45 %, respectively. The coefficient of correlation of the predicted CPUE with S.CPUE for the full GAM, GLM, GBM, CTA, and RF model was 0.456, 0.374, 0.471, 0.505, and 0.624, respectively. The RF model exhibited the highest performance in terms of R, the RMSE, and the MAE, with the CTA model having the second-highest performance. The GLM had the lowest performance in terms of R, the RMSE, and the MAE and also showed R value below 0.4 and therefore was not included in the subsequent analysis (Fig. 6b). No significant bias was observed in the performance of the selected single-algorithm models (Fig. 7) on the randomly split data set. The threefold CV results, which indicated that all of the selected single-algorithm models were reliable, was also validated by the results presented in Table 3 and incorporated for the development of the ensemble habitat model.

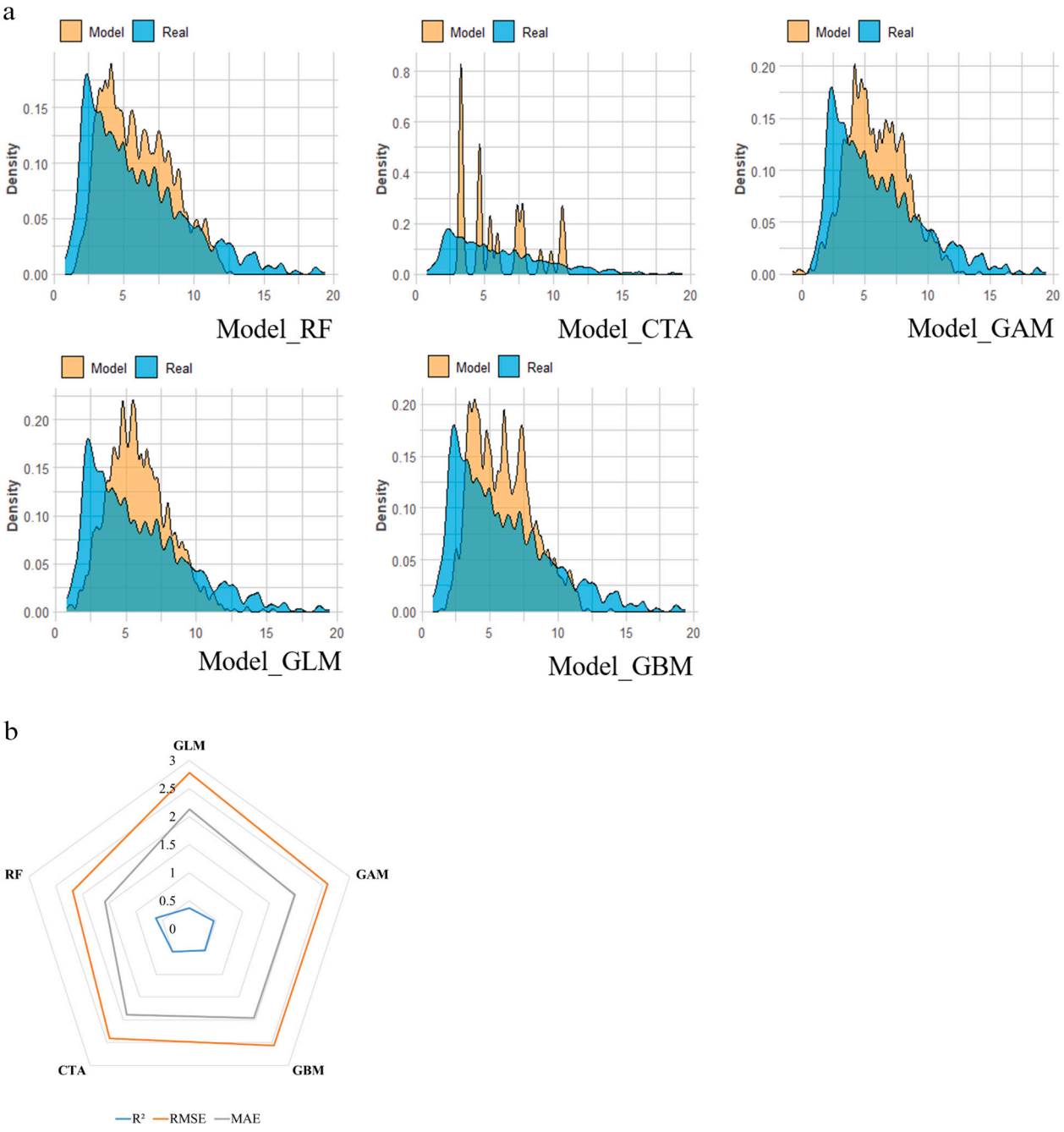

Fig. 6. a. Performance of the single-algorithm models.
b. Performance indices of the single-algorithm models.

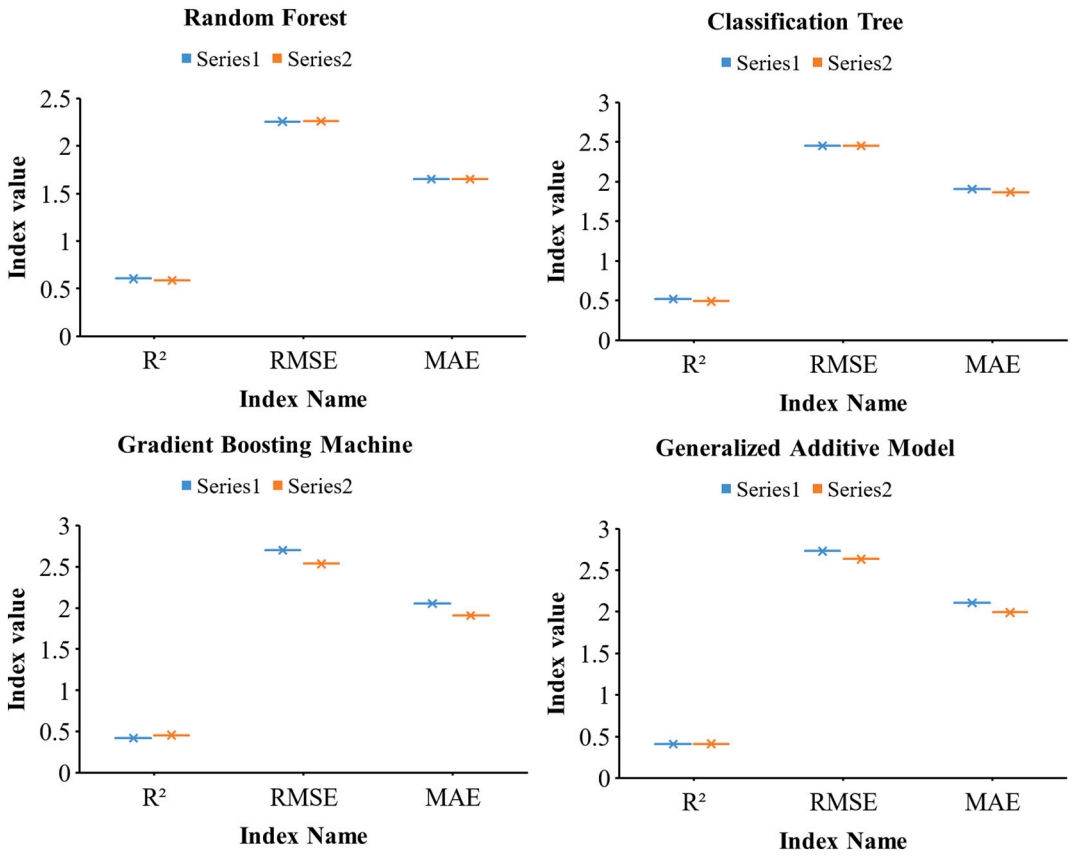

Fig. 7. Validation of the selected single-algorithm models. Series 1 and series 2 indicates 70 %, and 30 % data, respectively.

Table 3
Three-fold cross validation results of selected single-algorithm models.

CV-Run	GAM		GBM		RF		CTA	
	RMSE	*MAE*	*RMSE*	*MAE*	*RMSE*	*MAE*	*RMSE*	*MAE*
1	2.734	2.221	2.712	2.078	2.259	1.657	2.556	1.917
2	2.733	2.224	2.705	2.074	2.258	1.659	2.553	1.916
3	2.735	2.223	2.709	2.077	2.261	1.658	2.552	1.916

CV = Cross-validation; GAM = Generalized additive model; GBM = Gradient boosting machine; RF = Random forest; CTA = Classification and regression tree; RMSE = Root mean square error; MAE = Mean absolute error.

3.4. Comparison of single-algorithm and ensemble model performance

Comparison of the selected single-algorithm and the ensemble model performance depicted in Fig. 8. Among the selected single-algorithm models, RF model exhibited the least RMSE and MAE value of 2.259, and 1.657, respectively, followed by CTA, GBM, and GAM. The highest TSS, and AUC value was also exhibited by the RF model with value of 0.821, and 0.843, respectively, followed by CTA, GBM, and GAM. However, the RMSE, MAE, TSS, and AUC values of the ensemble habitat model were 1.021, 0.987, 0.888, and 0.921, respectively. This indicated the superior performance of the ensemble habitat model compared to all the selected single-algorithm models. Hence, the ensemble habitat model was incorporated for the subsequent analysis.

3.5. Seasonal ensemble prediction

No significant bias was discovered in relation to the predictive performance of the ensemble model (Table 4) after the threefold CV. Thus, the ensemble model was used to predict CPUE. The seasonal variation in the expected and standardized CPUE over the study period is shown in Fig. 9. In summer and fall, the Spanish mackerel distribution was mainly observed between 23° and 25°N and 117–118°E. After fall, the distribution shifted southward, extending to 22°N in the winter; the longitudinal area was restricted to 118°–119°E. The spring and summer distributions were similar, indicating a northward shift after winter. The latitudinal centers of gravity shifted southward after fall and then northward after winter (Fig. 10). The longitudinal centers of gravity shifted westward after summer and then eastward after winter.

4. Discussion

All of the single-algorithm models' estimated CPUE curves showed that the mean was less than the median. This indicated the negative skewness of the predicated CPUE curves. The predictive performance of all the models revealed RF as the best performing model for CPUE prediction, whereas, GLM was found as the least performing model. Moreover, all the machine learning models (GBM, CTA, and RF) showed better predictive performances than regression models (GLM, and GAM). This is because, machine learning models can deal better with complex and big datasets. Moreover, machine learning models may be less prone to skewed parameter estimates since they can be more resilient to outliers and noisy data. However, based on RMSE, MAE, AUC,

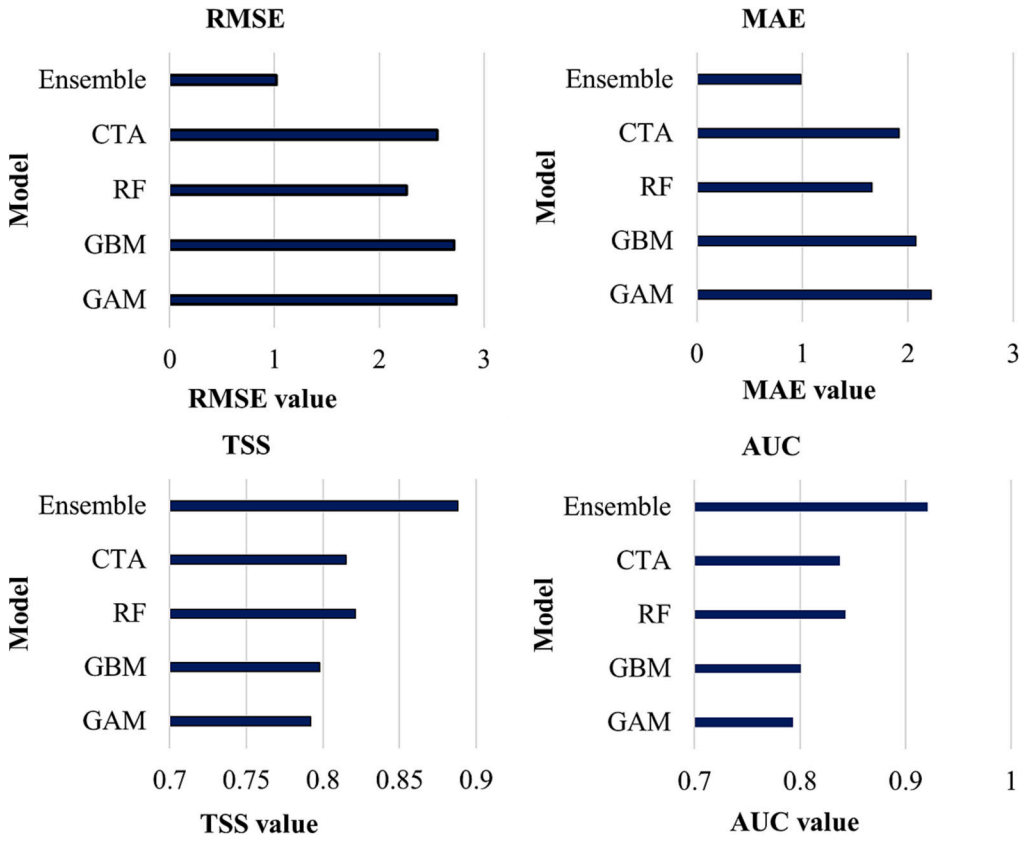

Fig. 8. Comparison of the selected single-algorithm and the ensemble model performance.

Table 4
Three-fold cross validation result of the ensemble model.

Metric	CV - Run 1	CV - Run 2	CV - Run 3
TSS	0.891	0.888	0.892
AUC	0.923	0.921	0.921

CV = Cross-validation; TSS = True skill statistics; AUC = Area under curve.

and TSS values, the ensemble habitat model's prediction ability in the current study was found to be superior to that of the selected single algorithm models. The superior performance of ensemble habitat models is explicable through a number of reasons. First, by merging numerous models, averaging or combining forecasts to balance errors from simplified models, and modeling sensitivity to minute data perturbations, ensembles lessen bias and variance in predictions (Alabia et al., 2020). Second, ensembles are excellent at transferring learning from training data to new data, identifying links and patterns that individual models would miss, and improving performance on brand-new cases (Dong et al., 2020). Third, ensembles, which combine multiple models, are less susceptible to overfitting due to their ability to smooth out individual errors and capture underlying patterns (Liu et al., 2023). Fourth, Ensembles reduce noise or outliers in data, resulting in more stable and reliable predictions due to less impact on individual models (Gong et al., 2021). The aforementioned explanations are sufficient to support the current finding, which shows that ensemble habitat model outperform single-algorithm models in terms of predictability also supported by previous studies (Mondal et al., 2023; Li and Wang, 2013; Alabia et al., 2016).

Ensemble prediction depicted that the narrow-barred Spanish mackerel are found near the Taiwan Bank throughout the year; this is likely attributable to the year-round presence of upwelling in the Taiwan Bank. During summer, Spanish mackerel mainly remain in the northwestern waters of the Taiwan Strait; by contrast, they are found in the southeastern waters during the winter. This could be because Spanish mackerel in the Taiwan Strait are spring spawners (Collette and Nauen, 1983). They migrate from early fall to late winter and aggregate in the central Taiwan Strait; hence, fall and winter are the two major fishing seasons in the Taiwan Bank (Tseng et al., 1971). The northeast monsoon (Jan et al., 2002) drives the cold China Coastal Current from the north to the southern part of the Taiwan Strait. This causes the migration of narrow-barred Spanish mackerel from early fall to late winter. According to Pankhurst and Munday (2011), increasing temperatures promote reproductive development in spring-spawning species. Hence, narrow-barred Spanish mackerel may tend to stay in cooler water because they are spring spawners. Our hypothesis is supported by the results presented in Table 2. This explains the preference of narrow-barred Spanish mackerel for cooler water in winter and spring. In spring, the southwest monsoon drives the warm South China Sea current from the southeast to northwest of the strait; following this current, Spanish mackerel migrate to the northwest after spring and until summer. A high SSC level indicates more abundant food. Table 2 indicates that in summer, the highest S.CPUE was in a region with a higher SSC level than that in spring. This may be because sufficient food must be available to sustain the larvae. Thus, Spanish mackerel tend to shift to the high-SSC warm northwestern waters of the Taiwan Strait after spawning in spring.

Oceanographic factors are key to the narrow-barred Spanish mackerel seasonal distributions in the Taiwan Strait. In the following, we mainly discussed the effects of two key predictors (the SST and SSC) on the narrow-barred Spanish mackerel's seasonal distribution. The SST is a key predictor of the relative frequency of any species in surface waters (Chen et al., 2005; Phillips et al., 2014; Arrizabalaga et al., 2015). The SST is also related to distribution limits of food supply which, is further related to the species' spatial distribution within these limits (Lan et al., 2018; Lee et al., 2020; Arrizabalaga et al., 2015; Dufour et al., 2010). The results of the present study clearly indicate that narrow-barred

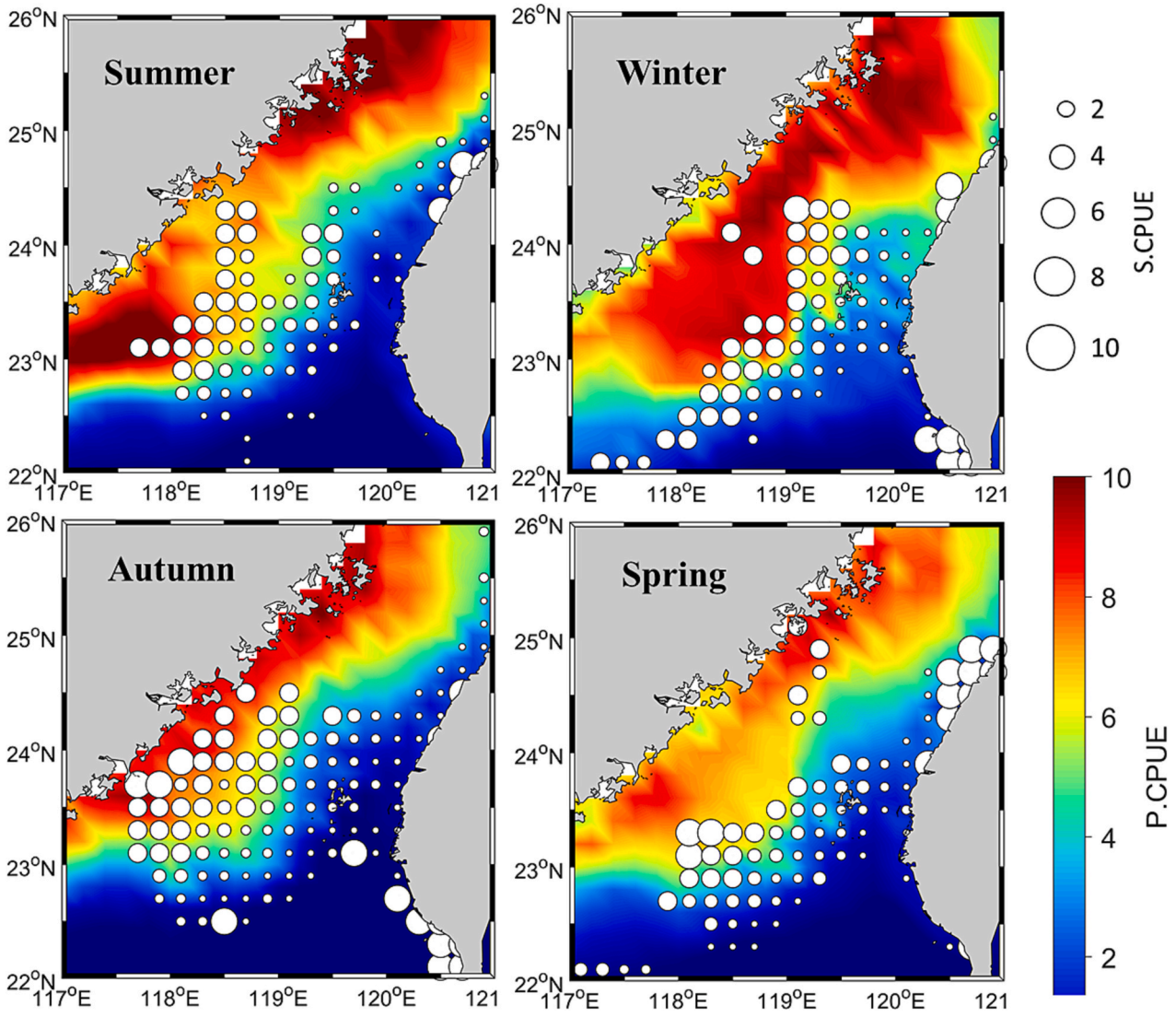

Fig. 9. Seasonal variation in the standardized and predicted CPUE.

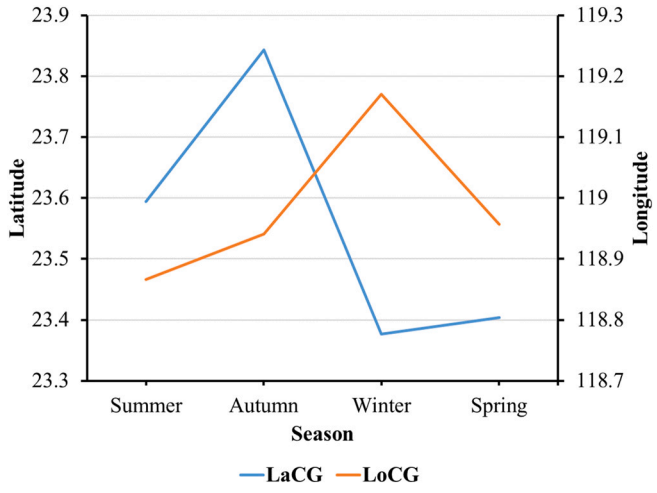

Fig. 10. Seasonal changes in the location of latitudinal and longitudinal centers of gravity of S.CPUE.

Spanish mackerel in the Taiwan Strait prefer the highest SST (25–26 °C) in the summer and lowest SST (16–17 °C) in the winter. Narrow-barred Spanish mackerel spawn in the spring; they therefore prefer a lower SST while spawning. After the spawning season (in the summer), they move to warmer areas to find enough food for their young (Chen et al., 2021; Weng et al., 2021). The SSC, a measure of phytoplankton density, attracts secondary producers which, is the diet of narrow-barred Spanish mackerel in the Taiwan Strait (Chen et al., 2009; Kumari et al., 2009; Vayghan et al., 2020). They prefer higher SSC levels (1.2–1.3 mg m^{-3}) in summer due to their faster metabolism, where secondary producers are higher, while lower levels (0.7–0.8 mg m^{-3}) are preferred in winter which, can be characterized by lower density of secondary producers due to slower metabolism. The preference for lower secondary producers density (lower SSC levels) in spring may be also due to almost no predation because of the insufficient energy of the fish after spawning, which may be another significant reason for their preference for lower SSC levels in spring than in other seasons. For marine species, salinity plays a key role in the critical process of osmoregulation (Dueri et al., 2014; Lignot and Charmantier, 2015; Telesh et al., 2013). Extreme variation in salt concentration may disrupt osmoregulation. Higher salinity also means higher water density, which can affect the speed of the water flow. For species that move frequently, such as Spanish mackerel, water currents are critical (Purba et al., 2021; Vayghan et al.,

2020). In some places, the SST affects both the MLD and SSH. de Boyer et al. (2004) found that when the SST decreases, the SSH decreases, causing the MLD to increase because of convection. This results in vertically diving fishes, such as Spanish mackerel, having a larger area in which they can dive to search for food.

One of the most significant species for commerce in the Taiwan Strait is the narrow-barred Spanish mackerel, although it has been threatened by depletion for a number of reasons. We hypothesize some explanations for the drop-in catch mainly after 2014. One factor that may have contributed to the observed phenomenon is the occurrence of El Nino episodes from May 2015 to May 2016 and from October 2018 to April 2019 as well as La Nina events from September 2016 to December 2016 and from October 2017 to April 2018 (Chen et al., 2021; Mammel et al., 2023). Certain combinations of water and wind may be harmful to animals because of the disruption to their habitats and the consequent decrease in feeding efficiency. Additionally, fish death may have occurred when the water temperature rose above or dropped below critical values during the El Nino or La Nina events, potentially resulting in the small fish catches after 2014. Another possible explanation for the phenomenon may have been a decrease in fishing activity, which may have resulted from the decline in the Spanish mackerel population in the Taiwan Strait (Taiwan Fisheries Agency, 2019; Ju et al., 2020). The populations of economically important species—such as the large yellow croaker, tiny yellow croaker, and hairtail—have been declining in the Taiwan Strait since the 1980s (Zhang et al., 2019). This may have been another key reason for the notable increase in the exploitation of narrow-barred Spanish mackerel resources, which in turn led to the emergence of early signs of overfishing in the 1990s. Overfishing can cause a decrease in the average length at maturity. Furthermore, the structure and function of marine ecosystems may have been jeopardized by the direct and indirect effects on nontarget species of human activity in numerous fisheries (Shepherd and Myers, 2005). The largest and most valuable species in an ecosystem are frequently the first to be targeted by fishermen, leading to their depletion to the point where fishing them is no longer profitable. Eventually, these fishermen shift their focus to smaller, now more profitable species that are lower down the food chain. The term “fishing down the food web” (Pauly et al., 1998) describes how overfishing can lead to changes in the ecosystem by reducing the biomass of economically significant species as well as the predators and prey of those species. Gillnet fisheries were shown to be the primary exploiters of narrow-barred Spanish mackerel in the Taiwan Strait, and the present findings suggest that reducing captures from this fishery might help decrease the vulnerability of bycatch species caught in gillnets.

By using data from the Taiwan Fishery Agency to develop an ensemble model, this study revealed how oceanographic changes are affecting the distribution and temporal variety of Spanish mackerel in the Taiwan Strait. A distinct southward shift of the distribution will likely occur in this region. The adaptive protection and management of fish habitats could be improved by leveraging knowledge regarding environmental refuges. SDMs can help locate productive fishing spots, identifying new fishing zones, reducing travel and fuel costs (Ntona and Morgera, 2018). However, overfishing can worsen if fishing grounds are easily accessible. Sustainable development goals (SDGs) aim to mitigate conditions like overfishing and climate change. SDMs can aid in conservation measures and species distribution in overfished areas, enabling adaptation of mitigation measures to align with SDGs (Friess et al., 2019; Fujii et al., 2021; Sturesson et al., 2018). SDMs can therefore be a very valuable tool for achieving the SDGs. For instant, the primary intent of SDG 14.4 is to maintain fish stocks at biologically sustainable levels. SDMs can facilitate this goal by identifying the existing or new habitats of narrow-barred Spanish mackerel in the Taiwan Strait. Moreover, SDG 14.5 is about protecting coastal and marine areas. Fishing could be temporarily banned in protected areas to maintain healthy fish stocks. SDG 14.6 states that subsidies for overfishing should be eliminated. Specifically, to stop overfishing, no subsidies should be provided to fishing boats that go to less-often-fished areas. Supporting the long-term health of the oceans and their resources can also be facilitated by improving scientific knowledge, research, and the sharing of marine technology. Related policies should consider the criteria and guidelines of the Intergovernmental Oceanographic Commission (SDG 14.a), support small-scale fisheries (SDG 14.b), and implement and uphold international maritime law (SDG 14.c). The first step in sustainability research might be modeling species' locations or habitats (Fig. 11). SDMs can facilitate these goals by identifying the existing or new habitats of narrow-barred Spanish mackerel in the Taiwan Strait. According to Ju et al. (2020), the Spanish mackerel population in the Taiwan Strait has significantly declined. Organizations responsible for fisheries management have developed and implemented ecosystem-based management strategies. Oceans may soon not be able to meet the needs of the species they contain (Neumann et al., 2019); thus, many individuals may have to dramatically reduce their usage of marine ecosystems. To sustain biologically suitable levels of species stock, understanding where and how narrow-barred Spanish mackerel prefer to live is critical (SDG 14.4). If enough people are aware of these habitats, the species could be protected (to meet SDG 14.6). In a future study, we intend to employ habitat-based modeling techniques to investigate the potential effects of climate change on narrow-barred Spanish mackerel populations to provide recommendations for promoting the long-term viability of this species in global climate change scenarios.

5. Conclusion

Interest in conservation efforts has increased as a result of the Taiwan Strait's declining stock of narrow-barred Spanish mackerel. It is critical to comprehend how they prefer their habitat in reaction to shifting surroundings in order to maximize conservation and restoration efforts. In this study, an ensemble modeling methodology was employed to investigate the influences of oceanographic factors on the seasonal distribution patterns of narrow-barred Spanish mackerel captured using gillnets in the Taiwan Strait. Winter was found to be the most productive season, with fall ranked second. The investigation also revealed that productivity levels of Spanish mackerel in the Taiwan Strait were lowest in summer. The predictive performance of all the models revealed RF as the best performing model for CPUE prediction. In summer and fall, the Spanish mackerel distribution was mainly observed between 23° and 25°N and 117–118°E. After fall, the distribution shifted southward, extending to 22°N in the winter; the longitudinal area was restricted to 118°–119°E. Following fall and spring, the location of the center of gravity of narrow-barred Spanish mackerel shifts substantially northward. The results of this research could greatly contribute to the attainment of numerous SDGs. For example, this information could reduce the time required to reach fishing areas, mitigate fishing pressure, augment economic viability, identify areas that are excessively fished as targets for potential restoration endeavors, and eventually increase the sustainability of fisheries.

CRediT authorship contribution statement

Conceptualization, S.M. and M.A.L.; methodology, M.A.L. and S.M.; software, S.M.; validation, M.A.L.; formal analysis, S.M.; investigation, M.A.L. and J.S.W.; resources, M.A.L.; writing (original draft preparation), S.M.; writing (review and editing), M.A.L and A.R.; visualization, K.E.O. and Y.K.C. All authors have read and approved of the published version of the manuscript.

Funding

This research was financed by the Council of Agriculture (111AS-6.4.2-FA-F1) and the National Science and Technology Council of Taiwan (NSTC111-2811-M-019-011).

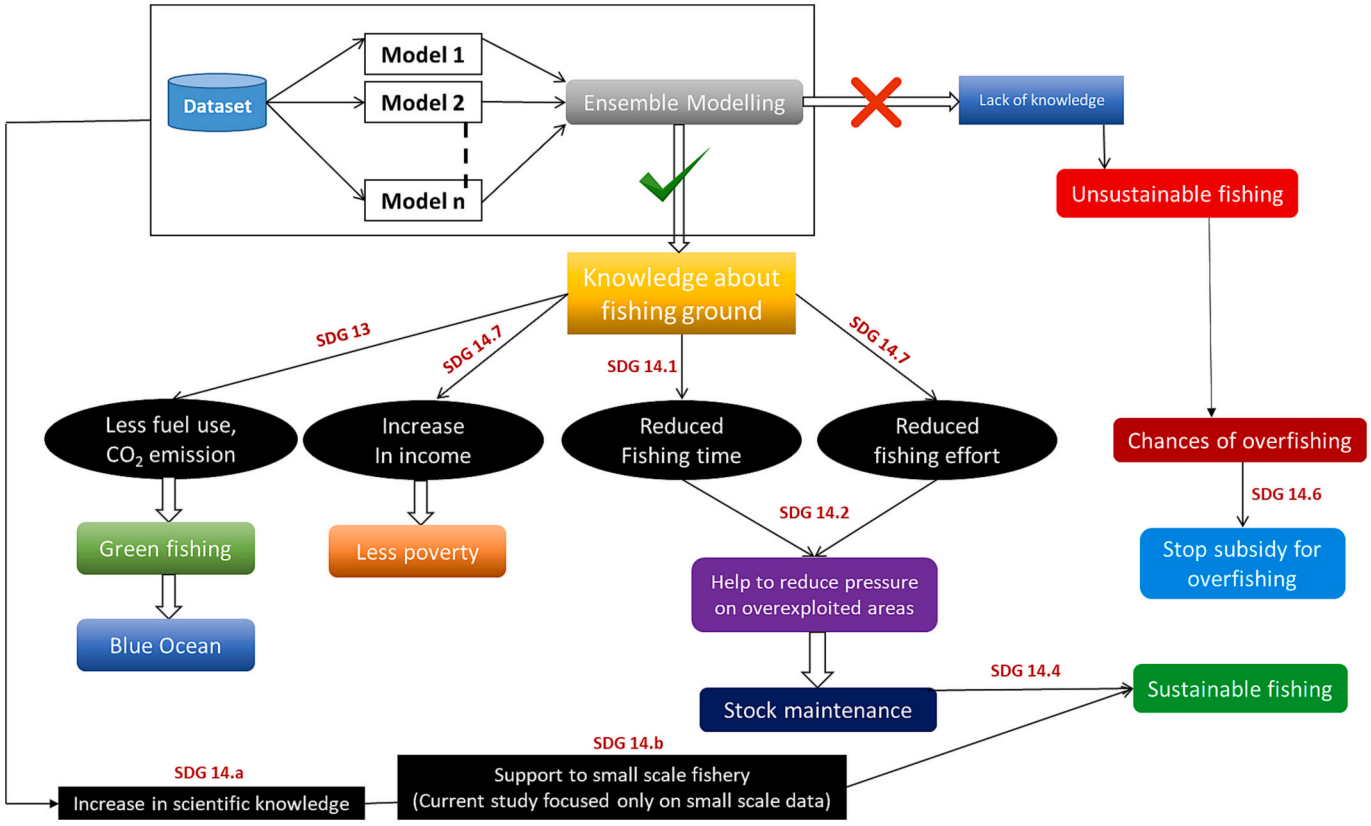

Fig. 11. Method of achieving SDG goals with the results of this study.

Declaration of competing interest

The authors declare that they have no known competing financial interests or personal relationships that could have appeared to influence the work reported in this paper.

Data availability

Data will be made available on request.

Acknowledgments

We thank the anonymous reviewers and editors for their valuable comments and suggestions as well as the team members of the Taiwan Fisheries Agency and National Science and Technology Council of Taiwan for their assistance in data preparation.

Appendix A. Supplementary data

Supplementary data to this article can be found online at https://doi.org/10.1016/j.marpolbul.2023.115733.

References

Ahmad, H., 2019. Machine learning applications in oceanography. Aquatic Research 2 (3), 161.
Alabia, I.D., Saitoh, S.I., Igarashi, H., Ishikawa, Y., Usui, N., Kamachi, M., Awaji, T., Seito, M., 2016. Ensemble squid habitat model using three-dimensional ocean data. ICES Journal of Marine Science 73 (7), 1863.
Alabia, I.D., Saitoh, S.I., Igarashi, H., Ishikawa, Y., Imamura, Y., 2020. Spatial habitat shifts of oceanic cephalopod (Ommastrephes bartramii) in oscillating climate. Remote Sens. (Basel) 12 (3), 521.
Arrizabalaga, H., Dufour, F., Kell, L., Merino, G., Ibaibarriaga, L., Chust, G., Irigoien, X., Santiago, J., Murua, H., Fraile, I., Chifflet, M., 2015. Global habitat preferences of commercially valuable tuna. Deep-Sea Res. II Top. Stud. Oceanogr. 113, 102–112.
Azzellino, A., Panigada, S., Lanfredi, C., Zanardelli, M., Airoldi, S., di Sciara, G.N., 2012. Predictive habitat models for managing marine areas: spatial and temporal distribution of marine mammals within the Pelagos Sanctuary (Northwestern Mediterranean sea). Ocean & coastal management 67, 63.
Báez, J.C., Czerwinski, I.A., Ramos, M.L., 2020. Climatic oscillations effect on the yellowfin tuna (Thunnus albacares) Spanish captures in the Indian Ocean. Fish. Oceanogr. 29 (6), 572.
Barman, Koushik Kanti, Bora, Swaroop Nandan, 2021a. Interaction of oblique water waves with a single chamber caisson type breakwater for a two-layer fluid flow over an elastic bottom. Ocean Eng. 238, 109766.
Barman, Koushik Kanti, Bora, Swaroop Nandan, 2021b. Scattering and trapping of water waves by a composite breakwater placed on an elevated bottom in a two-layer fluid flowing over a porous sea-bed. Appl. Ocean Res. 113, 102544.
Barman, Koushik Kanti, Bora, Swaroop Nandan, 2021c. Elastic bottom effects on ocean water wave scattering by a composite caisson-type breakwater placed upon a rock Foundation in a two-layer fluid. Int. J. Appl. Mech. 13, 2150114.
Barman, Koushik Kanti, Chanda, Ayan, Tsai, Chia-Cheng, 2023. A mathematical study of a two-layer fluid flow system in the presence of a floating breakwater in front of VLFS. App. Math. Model. 122, 706–730.
Barry, S., Elith, J., 2006. Error and uncertainty in habitat models. J. Appl. Ecol. 43 (3), 413–423.
Beale, C.M., Lennon, J.J., 2012. Incorporating uncertainty in predictive species distribution modelling. Philos. Trans. R. Soc., B 367 (1586), 247.
de Boyer, Montégut C., Madec, G., Fischer, A.S., Lazar, A., Iudicone, D., 2004. Mixed layer depth over the global ocean: an examination of profile data and a profile-based climatology. Journal of Geophysical Research: Oceans 109 (C12).
Charbonnel, A., Lambert, P., Lassalle, G., Quinton, E., Guisan, A., Mas, L., Paquignon, G., Lecomte, M., Acolas, M.L., 2023. Developing species distribution models for critically endangered species using participatory data: the European sturgeon marine habitat suitability. Estuar. Coast. Shelf Sci. 280, 108136.
Chen, I.C., Lee, P.F., Tzeng, W.N., 2005. Distribution of albacore (*Thunnus alalunga*) in the Indian Ocean and its relation to environmental factors. Fish. Oceanogr. 14 (1), 71–80.
Chen, X., Li, G., Feng, B., Tian, S., 2009. Habitat suitability index of Chub mackerel (Scomber japonicus) from July to September in the East China Sea. J. Oceanogr. 65 (1), 93.
Chen, L.C., Weng, J.S., Naimullah, M., Hsiao, P.Y., Tseng, C.T., Lan, K.W., Chuang, C.C., 2021. Distribution and catch rate characteristics of narrow-barred Spanish mackerel (*Scomberomorus commerson*) in relation to oceanographic factors in the waters around Taiwan. Front. Mar. Sci. 8, 770722.
Collette, B.B., Nauen, C.E., 1983. Scombrids of the World: An Annotated and Illustrated Catalogue Of Tunas, Mackerels, Bonitos, and Related Species Known to Date. v. 2.

Devi, G.K., Ganasri, B.P., Dwarakish, G.S., 2015. Applications of remote sensing in satellite oceanography: a review. Aquatic Procedia 4, 579.
Di Natale, A., El-Haweet, A.E.A., Abouelmagd, N., Lahoud, I., Bariche, M., 2020. Fisheries of the narrow-barred Spanish mackerel (Scomberomorus Commerson, Lacépède, 1800) in the southern and eastern Mediterranean Sea and relevance of this species to Iccat. Collect. Vol. Sci. Pap. Iccat 77 (9), 85.
Dong, J.Y., Hu, C., Zhang, X., Sun, X., Zhang, P., Li, W.T., 2020. Selection of aquaculture sites by using an ensemble model method: a case study of *Ruditapes philippinarums* in Moon Lake. Aquaculture 519, 734897.
Dueri, S., Bopp, L., Maury, O., 2014. Projecting the impacts of climate change on skipjack tuna abundance and spatial distribution. Glob. Chang. Biol. 20 (3), 742.
Dufour, F., Arrizabalaga, H., Irigoien, X., Santiago, J., 2010. Climate impacts on albacore and bluefin tunas migrations phenology and spatial distribution. Prog. Oceanogr. 86 (1–2), 283–290.
Dunn, A., Harley, S.J., Doonan, I.J., Bull, B., 2000. Calculation and interpretation of catch-per-unit effort (CPUE) indices. In: New Zealand Fisheries Assessment Report, 1, p. 44.
Friess, D.A., Aung, T.T., Huxham, M., Lovelock, C., Mukherjee, N., Sasmito, S., 2019. SDG 14: life below water–impacts on mangroves. Sustainable Development Goals 445, 445–481.
Fujii, I., Okochi, Y., Kawamura, H., 2021. Promoting cooperation of monitoring, control, and surveillance of IUU fishing in the Asia-Pacific. Sustainability 13 (18), 10231.
Gårdmark, A., Lindegren, M., Neuenfeldt, S., Blenckner, T., Heikinheimo, O., Müller-Karulis, B., Niiranen, S., Tomczak, M.T., Aro, E., Wikström, A., Möllmann, C., 2013. Biological ensemble modeling to evaluate potential futures of living marine resources. Ecol. Appl. 23 (4), 742–754.
Gong, C., Chen, X., Gao, F., Yu, W., 2021. The change characteristics of potential habitat and fishing season for neon flying squid in the northwest Pacific Ocean under future climate change scenarios. Marine and Coastal Fisheries 13 (5), 450–462.
Hazin, H.G., Hazin, F., Travassos, P., Carvalho, F.C., Erzini, K., 2007. Standardization of swordfish CPUE series caught by Brazilian longliners in the Atlantic Ocean, by GLM, using the targeting strategy inferred by cluster analysis. Collect. Vol. Sci. Pap. ICCAT 60 (6), 2039.
Hinton, M.G., Maunder, M.N., 2004. Methods for standardizing CPUE and how to select among them. Col. Vol. Sci. Pap. ICCAT 56 (1), 169.
Ho, C.H., Lu, H.J., He, J.S., Lan, K.-W., Chen, J.L., 2016. Changes in patterns of seasonality shown by migratory fish under global warming: evidence from catch data of Taiwan's coastal fisheries. Sustainability 8, 273.
Hobday, A.J., Pecl, G.T., 2014. Identification of global marine hotspots: sentinels for change and vanguards for adaptation action. Rev. Fish Biol. Fish. 24, 415.
Hossain, M.S., Sarker, S., Sharifuzzaman, S.M., Chowdhury, S.R., 2020. Primary productivity connects hilsa fishery in the Bay of Bengal. Sci. Rep. 10 (1), 1.
Hu, W., Du, J., Su, S., Tan, H., Yang, W., Ding, L., Dong, P., Yu, W., Zheng, X., Chen, B., 2022. Effects of climate change in the seas of China: predicted changes in the distribution of fish species and diversity. Ecol. Indic. 134, 108489.
Hysen, L., Nayeri, D., Cushman, S., Wan, H.Y., 2022. Background sampling for multi-scale ensemble habitat selection modeling: does the number of points matter? Eco. Inform. 72, 101914.
Jan, S., Wang, J., Chern, C.S., Chao, S.Y., 2002. Seasonal variation of the circulation in the Taiwan Strait. J. Mar. Syst. 35 (3–4), 249–268.
Ju, P., Cheung, W.W.L., Lu, Z., Yang, S., Guo, Z., Chen, M., et al., 2019. Age, growth, and abundance fluctuation of Jordan's damsel Teixeirichthys Jordani (Actinopterygii: Perciformes: Pomacentridae) in the southern Taiwan Strait. Acta Ichthyol. Piscat. 49, 243.
Ju, P., Tian, Y., Chen, M., Yang, S., Liu, Y., Xing, Q., Sun, P., 2020. Evaluating stock status of 16 commercial fish species in the coastal and offshore waters of Taiwan using the CMSY and BSM methods. Front. Mar. Sci. 7, 618.
Kuhn, M., 2008. Building predictive models in R using the caret package. J. Stat. Softw. 28, 1.
Kumari, B., Raman, M., Mali, K., 2009. Locating tuna forage ground through satellite remote sensing. Int. J. Remote Sens. 30 (22), 5977.
Lan, K.W., Lee, M.A., Chou, C.P., Vayghan, A.H., 2018. Association between the interannual variation in the oceanic environment and catch rates of bigeye tuna (Thunnus obesus) in the Atlantic Ocean. Fish. Oceanogr. 27 (5), 395–407.
Lan, X., Bai, J., Li, M., Li, J., 2020, October. Fish image classification using deep convolutional neural network. In: Proceedings of the 2020 International Conference on Computers, Information Processing and Advanced Education, pp. 18–22.
Lauridsen, T.L., Landkildehus, F., Jeppesen, E., Jørgensen, T.B., Søndergaard, M., 2008. A comparison of methods for calculating Catch Per Unit Effort (CPUE) of gill net catches in lakes. Fish. Res. 93 (1–2), 204.
Lee, M.A., Weng, J.S., Lan, K.W., Vayghan, A.H., Wang, Y.C., Chan, J.W., 2020. Empirical habitat suitability model for immature albacore tuna in the North Pacific Ocean obtained using multisatellite remote sensing data. International Journal of Remote Sensing 41 (15), 5819–5837.
Lehodey, P., Bertignac, M., Hampton, J., Lewis, A., Picaut, J., 1997. El Niño southern oscillation and tuna in the western Pacific. Nature 389, 715.
Lezama-Ochoa, N., Murua, H., Hall, M., Román, M., Ruiz, J., Vogel, N., Sancristobal, I., 2017. Biodiversity and habitat characteristics of the bycatch assemblages in fish aggregating devices (FADs) and school sets in the eastern Pacific Ocean. Front. Mar. Sci. 4, 265.
Li, X., Wang, Y., 2013. Applying various algorithms for species distribution modelling. Integrative zoology 8 (2), 124.
Li, G., Cao, J., Zou, X., Chen, X., Runnebaum, J., 2016. Modeling habitat suitability index for Chilean jack mackerel (Trachurus murphyi) in the south East Pacific. Fish. Res. 178, 47.
Liao, C.P., Huang, H.W., Lu, H.J., 2019. Fishermen's perceptions of coastal fisheries management regulations: key factors to rebuilding coastal fishery resources in Taiwan. Ocean Coast. Manag. 172, 1.
Lignot, J.H., Charmantier, G., 2015. Osmoregulation and excretion. In: The Natural History of Crustacean, vol. 4, p. 249.
Liu, S., Liu, Y., Li, J., Cao, C., Tian, H., Li, W., Tian, Y., Watanabe, Y., Lin, L., Li, Y., 2022. Effects of oceanographic environment on the distribution and migration of Pacific saury (Cololabis saira) during main fishing season. Sci. Rep. 12 (1), 13585.
Liu, S., Tian, Y., Liu, Y., Alabia, I.D., Cheng, J., Ito, S.I., 2023. Development of a prey-predator species distribution model for a large piscivorous fish: a case study for Japanese Spanish mackerel *Scomberomorus niphonius* and Japanese anchovy Engraulis japonicus. Deep-Sea Res. II Top. Stud. Oceanogr. 207, 105227.
Mammel, M., Lee, M.A., Naimullah, M., Liao, C.H., Wang, Y.C., Semedi, B., 2023. Habitat changes and catch rate variability for greater amberjack in the Taiwan Strait: the effects of El Niño–southern oscillation events. Front. Mar. Sci. 10, 1024669.
Mondal, S., Wang, Y.C., Lee, M.A., Weng, J.S., Mondal, B.K., 2022. Ensemble three-dimensional habitat modeling of Indian Ocean immature albacore tuna (*Thunnus alalunga*) using remote sensing data. Remote Sens. (Basel) 14 (20), 5278.
Mondal, S., Lee, M.A., Chen, Y.K., Wang, Y.C., 2023. Ensemble modeling of black Pomfret (*Parastromateus niger*) habitat in the Taiwan Strait based on oceanographic variables. PeerJ 11, e14990.
Neumann, B., Mikoleit, A., Bowman, J.S., Ducklow, H.W., Müller, F., 2019. Ecosystem service supply in the Antarctic Peninsula region: evaluating an expert-based assessment approach and a novel seascape data model. Front. Environ. Sci. 157.
Nguyen, K.Q., Nguyena, V.Y., 2017. Changing of sea surface temperature affects catch of Spanish mackerel *Scomberomorus commerson* in the set-net fishery. Fish. Aquac. J. 8, 231.
Niamaimandi, N., Kaymaram, F., Hoolihan, J.P., Mohammadi, G.H., Fatemi, S.M.R., 2015. Population dynamics parameters of narrow-barred Spanish mackerel, Scomberomorus commerson (Lacèpéde, 1800), from commercial catch in the northern Persian gulf. Global ecology and conservation 4, 666–672.
Ntona, M., Morgera, E., 2018. Connecting SDG 14 with the other Sustainable Development Goals through marine spatial planning. Mar. Policy 93, 214–222.
Pacifici, K., Reich, B.J., Miller, D.A., Gardner, B., Stauffer, G., Singh, S., Collazo, J.A., 2017. Integrating multiple data sources in species distribution modeling: a framework for data fusion. Ecology 98 (3), 840–850.
Pankhurst, N.W., Munday, P.L., 2011. Effects of climate change on fish reproduction and early life history stages. Mar. Freshw. Res. 62 (9), 1015–1026.
Pauly, D., Christensen, V., Dalsgaard, J., Froese, R., Torres Jr., F., 1998. Fishing down marine food webs. Science 279 (5352), 860–863.
Pearce, J., Ferrier, S., 2000. Evaluating the predictive performance of habitat models developed using logistic regression. Ecol. Model. 133 (3), 225–245.
Phillips, A.J., Ciannelli, L., Brodeur, R.D., Pearcy, W.G., Childers, J., 2014. Spatio-temporal associations of albacore CPUEs in the Northeastern Pacific with regional SST and climate environmental variables. ICES J. Mar. Sci. 71 (7), 1717–1727.
Purba, N.P., Faizal, I., Cordova, M.R., Abimanyu, A., Afandi, N.K., Indriawan, D., Khan, A.M., 2021. Marine debris pathway across Indonesian boundary seas. Journal of Ecological Engineering 22 (3), 82–98.
Ratner, B., 2009. The correlation coefficient: its values range between+ 1/− 1, or do they? J. Target. Meas. Anal. Mark. 17 (2), 139.
Reisinger, R.R., Raymond, B., Hindell, M.A., Bester, M.N., Crawford, R.J., Davies, D., de Bruyn, P.N., Dilley, B.J., Kirkman, S.P., Makhado, A.B., Ryan, P.G., 2018. Habitat modelling of tracking data from multiple marine predators identifies important areas in the Southern Indian Ocean. Divers. Distrib. 24 (4), 535.
Rew, J., Cho, Y., Moon, J., Hwang, E., 2020. Habitat suitability estimation using a two-stage ensemble approach. Remote Sens. (Basel) 12 (9), 1475.
Robinson, L.M., Elith, J., Hobday, A.J., Pearson, R.G., Kendall, B.E., Possingham, H.P., Richardson, A.J., 2011. Pushing the limits in marine species distribution modelling: lessons from the land present challenges and opportunities. Glob. Ecol. Biogeogr. 20 (6), 789.
Rowden, A.A., Anderson, O.F., Georgian, S.E., Bowden, D.A., Clark, M.R., Pallentin, A., Miller, A., 2017a. High-resolution habitat suitability models for the conservation and management of vulnerable marine ecosystems on the Louisville Seamount Chain, South Pacific Ocean. Front. Mar. Sci. 4, 335.
Rowden, A.A., Anderson, O.F., Georgian, S.E., Bowden, D.A., Clark, M.R., Pallentin, A., Miller, A., 2017b. High-resolution habitat suitability models for the conservation and management of vulnerable marine ecosystems on the Louisville Seamount Chain, South Pacific Ocean. Front. Mar. Sci. 4, 335.
Shepherd, T.D., Myers, R.A., 2005. Direct and indirect fishery effects on small coastal elasmobranchs in the northern Gulf of Mexico. Ecol. Lett. 8 (10), 1095–1104.
Stohlgren, T.J., Ma, P., Kumar, S., Rocca, M., Morisette, J.T., Jarnevich, C.S., Benson, N., 2010. Ensemble habitat mapping of invasive plant species. Risk Analysis 30 (2), 224.
Taiwan Fishery Agency report, (2019).
Sturesson, A., Weitz, N., Persson, Å., 2018. SDG 14: Life below water. A review of research needs. Technical annex to the Formas report Forskning för Agenda 2030. Översikt av forskningsbehov och vägar framåt. Stockholm Environment Institute, Stockholm.
Telesh, I., Schubert, H., Skarlato, S., 2013. Life in the salinity gradient: discovering mechanisms behind a new biodiversity pattern. Estuar. Coast. Shelf Sci. 135, 317.
Tian, S., Chen, X., Chen, Y., Xu, L., Dai, X., 2009. Standardizing CPUE of Ommastrephes bartramii for Chinese squid-jigging fishery in Northwest Pacific Ocean. Chinese J. Oceanol. Limnol. 27 (4), 729.
Tikhonov, G., Opedal, Ø.H., Abrego, N., Lehikoinen, A., de Jonge, M.M., Oksanen, J., Ovaskainen, O., 2020. Joint species distribution modelling with the R-package Hmsc. Methods Ecol. Evol. 11 (3), 442.

Tittensor, D.P., Eddy, T.D., Lotze, H.K., Galbraith, E.D., Cheung, W., Barange, M., Blanchard, J.L., Bopp, L., Bryndum-Buchholz, A., Büchner, M., Bulman, C., 2018. A protocol for the intercomparison of marine fishery and ecosystem models: fish-MIP v1. 0. Geosci. Model Dev. 11 (4), 1421–1442.

Tseng, W.Y., Chen, C.H., Hu, S.H., Chen, G.S., Pao, W.H., 1971. Preliminary study on Spanish mackerel of Taiwan. Bull. Taiwan Fish. Res. Institute 18, 89–114.

Vayghan, A.H., Lee, M.A., Weng, J.S., Mondal, S., Lin, C.T., Wang, Y.C., 2020. Multisatellite-based feeding habitat suitability modeling of albacore tuna in the southern Atlantic ocean. Remote Sens. (Basel) 12 (16), 2515.

Welliken, M.A., Pangaribuan, R.D., Melmambessy, E.H., Merly, S.L., Saleky, D., Sianturi, R., 2021. Spatial and temporal variation of sea surface temperature and chlorophyll-a on the mackerel fish (Scomberomorus commerson) distribution using aqua modis satellite in naukerjerai district, Merauke regency. In: Journal of Physics: Conference Series, IOP publishing, 1899(1), 012020.

Weng, J.S., Cheng, L.C., Lo, Y.S., Shiao, J.C., He, J.S., Lee, M.A., Liu, K.M., 2021. Demographics of Scomberomorus commerson in the Central Taiwan Strait. Journal of Marine Science and Engineering 9 (12), 1346.

Xing, Q., Yu, H., Liu, Y., Li, J., Tian, Y., Bakun, A., Cao, C., Tian, H., Li, W., 2022. Application of a fish habitat model considering mesoscale oceanographic features in evaluating climatic impact on distribution and abundance of Pacific saury (Cololabis saira). Prog. Oceanogr. 201, 102743.

Xue, Y., Guan, L., Tanaka, K., Li, Z., Chen, Y., Ren, Y., 2017. Evaluating effects of rescaling and weighting data on habitat suitability modeling. Fish. Res. 188, 84.

Yackulic, C.B., Chandler, R., Zipkin, E.F., Royle, J.A., Nichols, J.D., Campbell Grant, E.H., Veran, S., 2013. Presence-only modelling using MAXENT: when can we trust the inferences? Methods Ecol. Evol. 4 (3), 236–243.

Youssef, A.M., Pourghasemi, H.R., Pourtaghi, Z.S., Al-Katheeri, M.M., 2016. Landslide susceptibility mapping using random forest, boosted regression tree, classification and regression tree, and general linear models and comparison of their performance at Wadi Tayyah Basin, Asir Region, Saudi Arabia. Landslides 13 (5), 839.

Zhang, L., Zhou, Z., Li, H., Qiao, Y., Zhang, Y., 2019. The mitochondrial COI gene reveals the genetic diversity of chub mackerel (Scomber japonicus) in the Taiwan Strait and its adjacent waters. Pakistan J. Zool 51, 935–943.

Zhang, T., Song, L., Yuan, H., Song, B., Ebango Ngando, N., 2021. A comparative study on habitat models for adult bigeye tuna in the Indian Ocean based on gridded tuna longline fishery data. Fish. Oceanogr. 30 (5), 584.

Zimmermann, N.E., Edwards Jr., T.C., Graham, C.H., Pearman, P.B., Svenning, J.C., 2010. New trends in species distribution modelling. Ecography 33 (6), 985.

Zuur, A.F., Ieno, E.N., Elphick, C.S., 2010. A protocol for data exploration to avoid common statistical problems. Methods in Ecology and Evolution 1, 3.